**Supporting Information**

# Computational design of efficient and thermostable esterase for polylactic acid depolymerization

*Bin Xie[a,e#], Jun Zhang[c#], Huashan Sun[a,e], Rongrong Bai[a,e], Diannan Lu[c], Yushan Zhu[b], Weiliang Dong[a,d,e*], Zhou Jie[a,d,e*], Min Jiang[a,d,e]*

[a]State Key Laboratory of Materials-Oriented Chemical Engineering, College of Biotechnology and Pharmaceutical Engineering, Nanjing Tech University, Nanjing, 211800, P.R. China

[b]College of Life Science and Technology, National Energy R&D Center for Biorefinery, Beijing University of Chemical Technology, Beijing 100029, China

[c]Department of Chemical Engineering, Tsinghua University, Beijing 100084, China

[d]Jiangsu National Synergetic Innovation Center for Advanced Materials (SICAM), Nanjing Tech University, Nanjing 211800, P.R. China

[e]Key Laboratory for Waste Plastics Biocatalytic Degradation and Recycling, Nanjing Tech University, Nanjing 211816, Jiangsu, China

* Corresponding author: Jie Zhou, jayzhou@njtech.edu.cn;
Weiliang Dong, dwl@njtech.edu.cn

# Table of Contents

# Supporting Tables

**Table S1. Primers for designing single-point mutations.**

| Mutation Sites | Primer name | Sequence |
|---|---|---|
| S128Y | F-S128Y | CGACGGTtatATCGATCCGAAGATCCTGTTCA |
| | R-S128Y | GATCGATataACCGTCGAGACACATCCGCGCC |
| S153L | F-S153L | AGCTTCTTCctgCCTCTCGCCAAGATGCTGG |
| | R-S153L | AGAGGcagGAAGAAGCTCGCCGCCGG |
| P232A | F-P232A | AATCTGAAGgcgCTGCTGGTGCTGGTGGCG |
| | R-P232A | AGCAGcgcCTTCAGATTGGGTAACGCTTTCA |
| I245V | F-I245V | GCTgtgCCGCCATCGGTCGCGGTT |
| | R-I245V | ACCGATGGCGGcacAGCGCGGTCCCCCTCGGC |
| R276D | F-R276D | AGgatCCTGCGCTGATTGCCGCC |
| | R-R276D | AATCAGCGCAGGatcCTCCTCATGGGCCAGATGG |
| V202W | F-V202W | TGtggTCCAGCCCAAATCATGTCGCCGCAGCG |
| | R-V202W | ATTTGGGCTGGAccaCAGCTTGCCGTAGAGTTTGATCC |
| G139F | F-G139F | CCTCAATccaGCGTTTCTGCCCTATGGCGGCC |
| | R-G139F | GAAACGCtggATTGAGGCTGAACAGGATCTTCG |
| F151L | F-F151L | AGCctaTTCTCGCCTCTCGCCAAGATGCTGGT |
| | R-F151L | AGAGGCGAGAAtagGCTCGCCGCCGGGCCGCC |
| A267G | F-A267G | ATTCCGggtCTCGGCCATCTGGCCCATGAGGA |
| | R-A267G | TGGCCGAGaccCGGAATCCGCTCGATCACCGC |

**Table S2-1. Potentially stabilizing mutations predicted by PROSS[1] calculations.**

| Number | Wild Type | design_1 | design_2 | design_3 | design_4 | design_5 | design_6 | design_7 | design_8 | design_9 | Variant |
|---|---|---|---|---|---|---|---|---|---|---|---|
| 282 | A | | | | | | | | | E | A282E |
| 255 | E | | | | | | | | | A | E255A |
| 285 | E | | | | | | | | | R | E285R |
| 161 | M | | | | | | | | | L | M161L |
| 276 | R | | | | | | | | | D | R276D |
| 128 | S | | | | | | | | | M | S128M |
| 248 | S | | | | | | | | | D | S248D |
| 102 | V | | | | | | | | | A | V102A |
| 233 | L | | | | | | | | P | P | L233P |
| 261 | V | | | | | | | | R | R | V261R |
| 22 | I | | | | | | | V | V | V | I22V |
| 225 | K | | | | | | | R | R | R | K226R |
| 150 | S | | | | | | | R | R | R | S150R |
| 203 | S | | | | | | | Q | Q | Q | S203Q |
| 251 | V | | | | | | | E | E | R | V251R |
| 254 | R | | | | | | A | A | A | A | R254A |
| 94 | S | | | | | | E | E | E | E | S94E |
| 134 | L | I | I | | I | | | | I | | L134I |
| 221 | E | | | | | D | D | D | D | D | E221D |

| | | | | | | | | | | | |
|---|---|---|---|---|---|---|---|---|---|---|---|
| 11 | L | | | | | R | R | R | R | R | L11R |
| 176 | R | | | | | P | P | P | P | P | R176P |
| 167 | S | | | | | H | H | H | H | H | S167H |
| 241 | G | | Q | Q | Q | Q | | | Q | Q | G241Q |
| 265 | I | | | | L | L | L | L | L | L | I265L |
| 196 | K | | | | A | A | A | A | A | A | K196A |
| 159 | L | | | | M | M | M | M | M | M | L159M |
| 206 | N | | | | G | G | H | H | H | H | N206H |
| 154 | P | | A | A | A | A | A | A | A | A | P154A |
| 36 | S | | D | D | D | D | D | D | D | D | S36D |
| 193 | A | R | R | R | R | R | R | R | R | R | A193R |
| 238 | A | V | V | V | V | V | V | V | V | V | A238V |
| 267 | A | G | G | G | G | G | G | G | G | G | A267G |
| 38 | A | D | D | D | D | D | D | D | D | D | A38D |
| 151 | F | L | L | L | L | L | L | L | L | L | F151L |
| 139 | G | P | P | P | P | P | P | P | P | P | G139P |
| 222 | P | T | T | T | T | T | T | T | T | T | P222T |
| 232 | P | A | A | V | A | V | V | V | V | V | P232V |
| 160 | V | A | A | A | A | A | A | A | A | A | V160A |

**Table S2-2. Potentially stabilizing mutations predicted by Fireprot[2] calculations.**

| Combined mutant: −35.20 kcal/mol (16 mutations) | | | | | | | |
|---|---|---|---|---|---|---|---|
| Chain | Mutation | Conserved | Correlated | BTC by majority | BTC by ratio | FoldX(kcal/mol) | Rosetta(kcal/mol) |
| A | I45L | Y | N | Y | N | 0.12 | - |
| A | S63A | N | N | Y | Y | 0.22 | - |
| A | Y66F | Y | N | Y | N | -0.61 | - |
| A | Q104G | N | N | N | Y | -0.86 | - |
| A | S128Y | N | N | N | N | -2.4 | -2.75 |
| A | Y144F | Y | N | Y | Y | 0.4 | - |
| A | F151L | N | N | Y | Y | -0.09 | - |
| A | S153L | N | N | N | N | -1.49 | -2.52 |
| A | A173Y | N | N | N | N | -2.15 | -3.66 |
| A | G199Y | N | N | N | N | -1.55 | -5.27 |
| A | K200R | N | N | Y | Y | 0.03 | - |
| A | V202W | N | N | N | N | -1.57 | -4.34 |
| A | A209W | N | N | N | N | -1.64 | -2.33 |
| A | I245V | Y | N | Y | N | 0.44 | - |
| A | A267G | N | N | Y | Y | -2.3 | -2.96 |
| A | A281Y | N | N | N | N | -1.3 | -4.73 |
| Energy mutant: −33.75 kcal/mol (8 mutations) | | | | | | | |
| Chain | Mutation | Conserved | Correlated | FoldX(kcal/mol) | Rosetta(kcal/mol) | | |

| | | | | | |
|---|---|---|---|---|---|
| A | S128Y | N | N | -2.4 | -2.75 |
| A | S153L | N | N | -1.49 | -2.52 |
| A | A173Y | N | N | -2.15 | -3.66 |
| A | G199Y | N | N | -1.55 | -5.27 |
| A | V202W | N | N | -1.57 | -4.34 |
| A | A209W | N | N | -1.64 | -2.33 |
| A | A267G | N | N | -2.3 | -2.96 |
| A | A281Y | N | N | -1.3 | -4.73 |

Evolution mutant: −2.96 kcal/mol (9 mutations)

| Chain | Mutation | BTC by majority | BTC by ratio | FoldX(kcal/mol) |
|---|---|---|---|---|
| A | I45L | Y | N | 0.12 |
| A | S63A | Y | Y | 0.22 |
| A | Y66F | Y | N | -0.61 |
| A | Q104G | N | Y | -0.86 |
| A | Y144F | Y | Y | 0.4 |
| A | F151L | Y | Y | -0.09 |
| A | K200R | Y | Y | 0.03 |
| A | I245V | Y | N | 0.44 |
| A | A267G | Y | Y | -2.3 |

**Table S2-3. Potentially stabilizing mutations predicted by GRAPE[3] calculations, based respectively on FoldX, Rosetta, ABACUS method.**

| Chain | WT | MUT | Num | Energy | SD | Method | WTNumMUT |
|---|---|---|---|---|---|---|---|
| A | A | D | 18 | -2.428 | 0.064 | FoldX | A18D |
| A | R | L | 83 | -2.128 | 0.111 | FoldX | R83L |
| A | A | M | 38 | -2.066 | 0.075 | FoldX | A38M |
| A | L | E | 11 | -1.941 | 0.015 | FoldX | L11E |
| A | P | M | 14 | -1.905 | 0.008 | FoldX | P14M |
| A | T | L | 81 | -1.885 | 0.12 | FoldX | T81L |
| A | S | L | 63 | -1.869 | 0.044 | FoldX | S63L |
| A | V | R | 31 | -1.776 | 0.146 | FoldX | V31R |
| A | Q | W | 80 | -1.635 | 0.023 | FoldX | Q80W |
| A | P | V | 60 | -1.597 | 0.228 | FoldX | P60V |
| A | D | V | 95 | -1.511 | 0.042 | FoldX | D95V |
| A | L | G | 86 | -1.51 | 0.029 | FoldX | L86G |
| A | G | E | 77 | -1.505 | 0.036 | FoldX | G77E |
| A | G | T | 26 | -1.494 | 0.092 | FoldX | G26T |
| A | Y | P | 66 | -1.452 | 0.052 | FoldX | Y66P |
| A | L | Q | 61 | -1.412 | 0.082 | FoldX | L61Q |
| A | P | T | 37 | -1.358 | 0.384 | FoldX | P37T |
| A | A | I | 97 | -1.347 | 0.008 | FoldX | A97I |
| A | P | N | 40 | -1.346 | 0.197 | FoldX | P40N |
| A | L | Q | 62 | -1.332 | 0.065 | FoldX | L62Q |
| A | H | W | 30 | -1.321 | 0.032 | FoldX | H30W |
| A | W | H | 29 | -1.275 | 0.589 | FoldX | W29H |
| A | D | L | 9 | -1.263 | 0.002 | FoldX | D9L |
| A | G | I | 57 | -1.257 | 0.345 | FoldX | G57I |
| A | P | S | 82 | -1.245 | 0.011 | FoldX | P82S |
| A | L | Y | 4 | -1.227 | 0.006 | FoldX | L4Y |
| A | E | V | 17 | -1.199 | 0.009 | FoldX | E17V |
| A | V | S | 69 | -1.188 | 0.106 | FoldX | V69S |
| A | F | S | 78 | -1.179 | 0.046 | FoldX | F78S |
| A | S | W | 94 | -1.155 | 0.012 | FoldX | S94W |
| A | A | E | 70 | -1.139 | 0.156 | FoldX | A70E |
| A | L | T | 96 | -1.129 | 0.079 | FoldX | L96T |
| A | H | F | 76 | -1.081 | 0.052 | FoldX | H76F |
| A | G | F | 25 | -1.074 | 0.063 | FoldX | G25F |
| A | H | S | 15 | -1.065 | 0.116 | FoldX | H15S |
| A | S | Q | 36 | -1.022 | 0.206 | FoldX | S36Q |
| A | H | V | 65 | -1.022 | 0.017 | FoldX | H65V |

| Chain | WT | MUT | Num | Energy | SD | Method | WTNumMUT |
|---|---|---|---|---|---|---|---|
| A | R | P | 83 | -30.476 | 0.014 | Rosetta | R83P |
| A | P | W | 154 | -13.757 | 0.005 | Rosetta | P154W |
| A | P | Q | 222 | -11.069 | 0 | Rosetta | P222Q |
| A | P | I | 166 | -10.38 | 0 | Rosetta | P166I |
| A | S | L | 153 | -9.901 | 0.027 | Rosetta | S153L |
| A | P | A | 232 | -8.371 | 0 | Rosetta | P232A |
| A | S | Y | 128 | -8.215 | 0 | Rosetta | S128Y |
| A | E | L | 221 | -7.501 | 0 | Rosetta | E221L |
| A | V | W | 202 | -7.363 | 0.114 | Rosetta | V202W |
| A | G | F | 145 | -7.053 | 0.006 | Rosetta | G145F |
| A | A | F | 238 | -6.877 | 0 | Rosetta | A238F |
| A | M | F | 84 | -6.544 | 0 | Rosetta | M84F |
| A | D | Y | 95 | -6.532 | 0 | Rosetta | D95Y |
| A | K | L | 231 | -6.319 | 0 | Rosetta | K231L |
| A | M | W | 34 | -6.288 | 0 | Rosetta | M34W |
| A | A | W | 173 | -6.269 | 0 | Rosetta | A173W |
| A | G | F | 199 | -6.24 | 1.256 | Rosetta | G199F |
| A | G | P | 139 | -6.224 | 0.03 | Rosetta | G139P |
| A | G | F | 241 | -6.125 | 0.01 | Rosetta | G241F |
| A | A | W | 156 | -5.953 | 0 | Rosetta | A156W |
| A | G | Y | 57 | -5.808 | 0.183 | Rosetta | G57Y |
| A | G | D | 91 | -5.808 | 0 | Rosetta | G91D |
| A | H | F | 53 | -5.712 | 0.002 | Rosetta | H53F |
| A | R | F | 264 | -5.61 | 0 | Rosetta | R264F |
| A | A | W | 149 | -5.517 | 0.694 | Rosetta | A149W |
| A | G | R | 184 | -5.37 | 0 | Rosetta | G184R |
| A | T | P | 48 | -5.344 | 0.004 | Rosetta | T48P |
| A | E | W | 285 | -5.297 | 0 | Rosetta | E285W |
| A | G | F | 49 | -5.248 | 0.001 | Rosetta | G49F |
| A | R | W | 122 | -5.23 | 0 | Rosetta | R122W |
| A | A | Y | 106 | -5.22 | 0 | Rosetta | A106Y |
| A | K | W | 196 | -5.173 | 0.007 | Rosetta | K196W |

| Chain | WT | MUT | Num | Energy | SD | Method | WTNumMUT |
|---|---|---|---|---|---|---|---|
| A | Q | D | 108 | -16.567 | 0 | ABACUS | Q108D |
| A | T | S | 79 | -9.675 | 0 | ABACUS | T79S |
| A | G | L | 139 | -7.408 | 0 | ABACUS | G139L |
| A | A | L | 288 | -6.784 | 0 | ABACUS | A288L |
| A | E | I | 263 | -6.769 | 0 | ABACUS | E263I |
| A | K | D | 132 | -6.402 | 0 | ABACUS | K132D |
| A | S | D | 136 | -6.367 | 0 | ABACUS | S136D |
| A | P | A | 166 | -5.95 | 0 | ABACUS | P166A |
| A | A | N | 51 | -5.614 | 0 | ABACUS | A51N |
| A | A | G | 239 | -5.279 | 0 | ABACUS | A239G |
| A | A | G | 117 | -5.117 | 0 | ABACUS | A117G |
| A | A | T | 41 | -5.11 | 0 | ABACUS | A41T |
| A | F | L | 141 | -4.774 | 0 | ABACUS | F141L |
| A | H | Q | 273 | -4.634 | 0 | ABACUS | H273Q |
| A | L | A | 120 | -4.586 | 0 | ABACUS | L120A |
| A | D | L | 126 | -4.543 | 0 | ABACUS | D126L |
| A | G | L | 194 | -4.449 | 0 | ABACUS | G194L |
| A | S | L | 128 | -4.315 | 0 | ABACUS | S128L |
| A | Y | L | 198 | -4.27 | 0 | ABACUS | Y198L |
| A | F | L | 135 | -4.269 | 0 | ABACUS | F135L |
| A | N | S | 138 | -4.196 | 0 | ABACUS | N138S |
| A | R | D | 276 | -3.757 | 0 | ABACUS | R276D |
| A | F | A | 152 | -3.717 | 0 | ABACUS | F152A |
| A | H | A | 175 | -3.58 | 0 | ABACUS | H175A |
| A | G | F | 10 | -3.544 | 0 | ABACUS | G10F |
| A | I | V | 245 | -3.537 | 0 | ABACUS | I245V |
| A | H | V | 207 | -3.434 | 0 | ABACUS | H207V |
| A | Q | Y | 32 | -3.288 | 0 | ABACUS | Q32Y |
| A | W | I | 6 | -3.256 | 0 | ABACUS | W6I |
| A | S | W | 52 | -3.224 | 0 | ABACUS | S52W |
| A | R | T | 28 | -3.223 | 0 | ABACUS | R28T |
| A | F | E | 164 | -3.151 | 0 | ABACUS | F164E |
| A | Y | P | 144 | -3.12 | 0 | ABACUS | Y144P |
| A | W | L | 29 | -3.113 | 0 | ABACUS | W29L |
| A | L | I | 236 | -3.041 | 0 | ABACUS | L236I |

**Table S3. Structural basis and effect on thermostability of the single mutations for experimental tests predicted by three stability prediction tools.**

| Mutations | Orgin [a] | Location | Predicted improvement |
|---|---|---|---|
| S128Y | FireProt/GRAPE | loop in Hyd [b] | New H-bond interactions with the hydroxy Oxygen S94 |
| G139P | PROSS/GRAPE | loop connecting Lid and Hyd | Increase of the rigidity of the loop |
| F151L | PROSS/FireProt | α-helix in Lid | Reduction of unfavorable hydrophobic buildup on exposed surfaces |
| S153L | FireProt/GRAPE | α-helix in Lid | Hydrophobic interactions |
| V202W | FireProt/GRAPE | α-helix in Lid | Entropic stabilization + Optimized surface charge<br>Hydrophobic interactions and filling the deeply buried cavity |
| P232A | PROSS/GRAPE | loop in Hyd | Enhanced local hydrophobic packing |
| I245V | FireProt/GRAPE | loop in Hyd | Based on evolutionary information |
| A267G | PROSS/FireProt | loop in Hyd | Reduction of exclusion with P266 |
| R276D | PROSS/GRAPE | α-helix in Hyd | New H-bond with backbone nitrogens of A278 and L279 |

[a] Single mutations predicted by at least two tools simultaneously were selected for experimental tests.

[b] The hydrolase domain is abbreviated as Hyd and the lid domain as Lid.

**Table S4.** Overall scoring ranking of three mutations predicted by three predictive tools for disulfide bonds. The tools used to predict disulfide bond mutations were: Yosshi[4], MAESTROweb[5], and SSbondPre[6].

| Predicted mutations | Yosshi's Rank | MAESTROwe' Rank | SSbondPre's Rank |
|---|---|---|---|
| M34-S63 | 22/59 | 2/106 | 13/51 |
| A97-S128 | 35/59 | 1/106 | 9/51 |
| L257-A260 | 17/59 | 41/106 | 50/51 |
| A51-G77 | 1/59 | 25/106 | |

**Table S5. Folding free energy changes of experimental variants computed by Cartesian_ddg[7].**

| Mutation | $\Delta\Delta G_{fold}$ (kcal/mol)[a] |
|---|---|
| S128Y | -8.46 |
| G139P | -4.79 |
| F151L | -1.53 |
| S153L | -9.76 |
| V202W | -7.47 |
| P232A | -9.14 |
| I245V | **1.63** [b] |
| A267G | -3.32 |
| R276D | -0.56 |
| F151L/A267G | -4.86 |
| I245V/R276D | **1.05** [b] |
| I245V/S128Y | -6.66 |
| S153L/R276D | -10.34 |
| S153L/S128Y | -18.22 |
| S153L/I245V | -7.68 |
| S153L/I245V/R276D | -8.59 |
| S153L/I245V/R276D/S128Y | -17.05 |
| S153L/I245V/S128Y/V202W | -23.70 |
| S153L/I245V/R276D/S128Y/V202W | -24.51 |

[a] $\Delta\Delta G_{fold}$ is the difference of the folding energy of variant minus that of wild type. The value is the average of three rounds of Cartesian_ddg calculations.

[b] The only two variants with positive $\Delta\Delta G_{fold}$, because I245V is a conserved mutation provided by evolutionary information.

**Table S6. Kinetic parameters of R5, WT derived from Michaelis-Menten experiments with 1-naphthylpropionate as substrate.**

| Protein | $V_{max}$（μmol/min/mg） | $K_m$(mM) | $K_{cat}$ ($S^{-1}$) | $K_{cat}/K_m$($S^{-1}mM^{-1}$) |
|---|---|---|---|---|
| WT | 2.22±0.11 | 0.74±0.1 | 1.17±0.06 | 1.59 |
| R5 | 4.28±0.20 | 0.71±0.09 | 2.26±0.11 | 3.19 |

**Table S7. Kinetic parameters of R5, WT derived from the inverse Michaelis-Menten experiments[8] with PDLLA substrate concentration fixed at 10 g/L.**

| Protein | $^{Inv}V_{max}$/S (μmol $g^{-1}$ $s^{-1}$) | $^{Inv}K_m$($mg_{enzyme}$ $g_{PLA}^{-1}$) |
|---|---|---|
| WT | 0.1913 | 1.6380 |
| R5 | 0.9229 | 1.1710 |

# Supporting Figures

**Figure S1.** SDS-PAGE[9] validation of the wild-type protein after single-point mutation. (A) The protein purification bands of V202W, S128Y, P232A crude enzyme extracts, along with S153L, R276D, and I245V. Notably, no corresponding protein band was found for the P232A mutation. (B) The protein purification bands for G139P, F151L, and A267G.

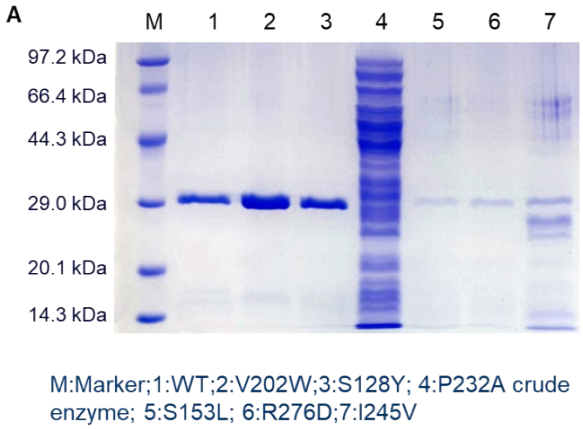


M:Marker;1:WT;2:V202W;3:S128Y; 4:P232A crude enzyme; 5:S153L; 6:R276D;7:I245V

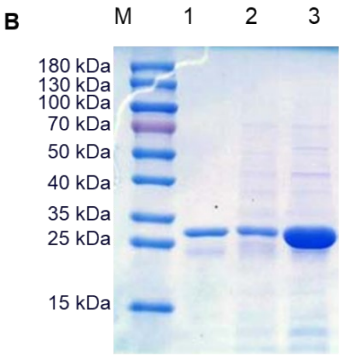


M:180 kDa Marker;1:G139P;2:F151L; 3:A267G.

**Figure S2.** Optimization of the enzymatic activity assay system for 1-naphthylpropionate[10]. (A) Visible light wavelength scan of the product 1-naphthylpropionate formed after the reaction. Under alkaline conditions, the released product 1-

naphthol undergoes a catalytic reaction with ferricyanide in the presence of 4-aminoantipyrine, yielding a purple-red product with maximum absorption at a wavelength of 510 nm. (B) Standard curve established with different concentrations of 1-naphthol. (C)Absorbance intensity at 510 nm after 10 min reaction with 1-naphthylpropionate at different temperatures. (D) Absorbance intensity at 510 nm at different time points during the reaction with 1-naphthylpropionate. (E) Absorbance intensity at 510 nm after the reaction of different enzyme concentrations with 1-naphthylpropionate.

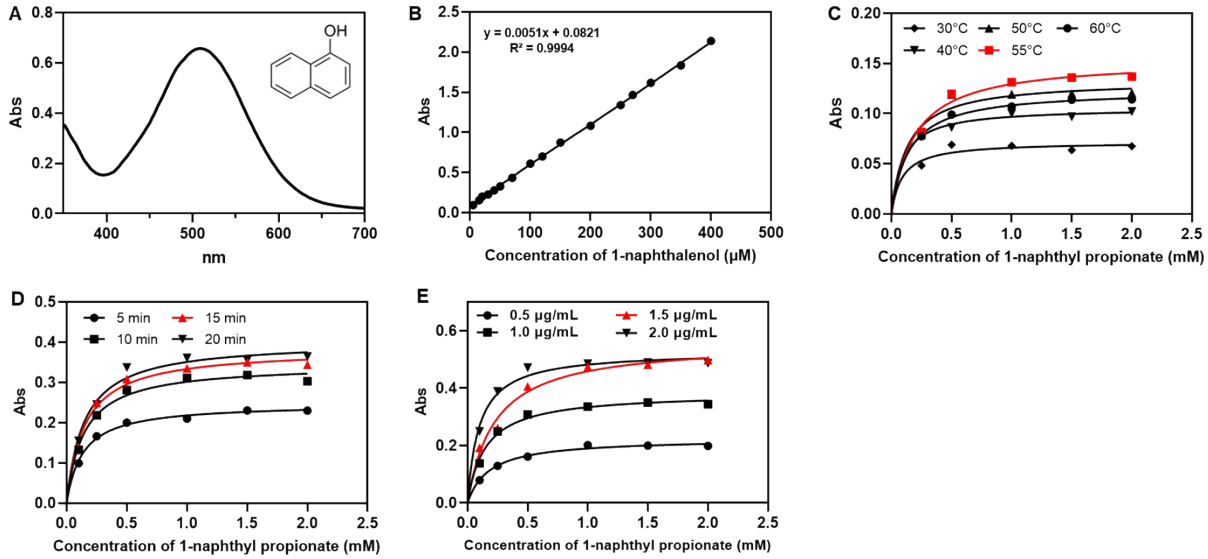


**Figure S3.** (A) Validation of the purified protein after disulfide bond combinatorial mutation with SDS-PAGE. (B) Evaluation of the enzyme activity of the mutants using 1-naphthyl propionate as a soluble substrate at 55°C. (C) Evaluation of the thermal stability of mutants after heat treatment at different temperatures for 30 min. (D) Evaluation of the thermal

stability of mutants after heat treatment at different temperatures for 60 min. Residual enzyme activity was assessed using 1-naphthyl propionate, with enzyme hydrolysis monitored by measuring absorbance at a wavelength of 510 nm.

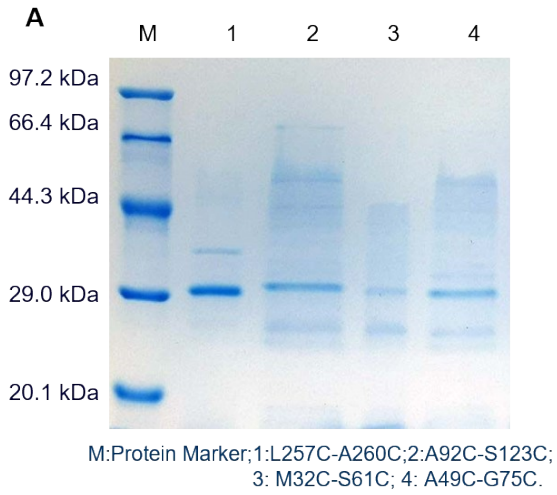


M:Protein Marker;1:L257C-A260C;2:A92C-S123C;
3: M32C-S61C; 4: A49C-G75C.

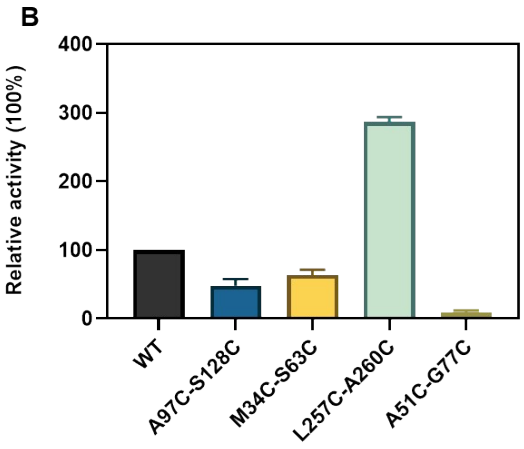


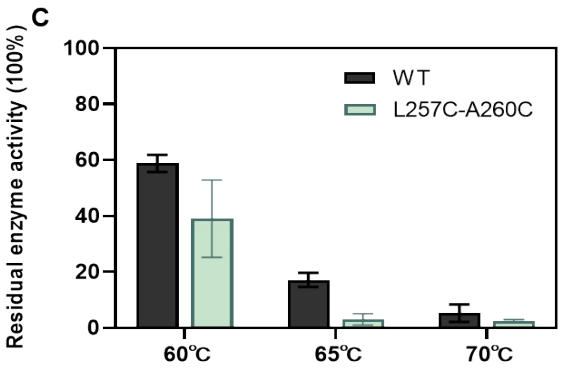


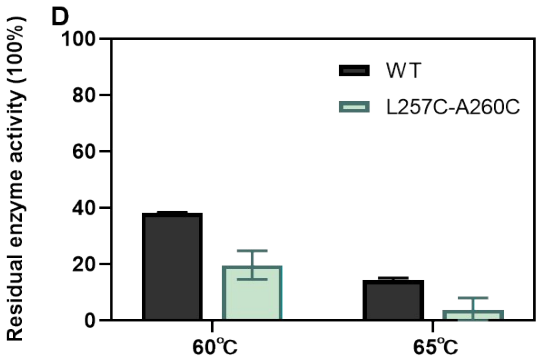

**Figure S4.** Comparison of the thermal stability properties between the mutants and the wild type (WT). (A) Fluorescence curves of all mutant proteins in DSF [11](differential scanning fluorimetry) to calculate the temperature at which the fluorescence signal rises by half ($T_m$). (B) Comparison of the thermal stability between variant R5 and WT after heat treatment at different temperatures for different minutes. 1-naphthylpropionate was used as the detection substrate.

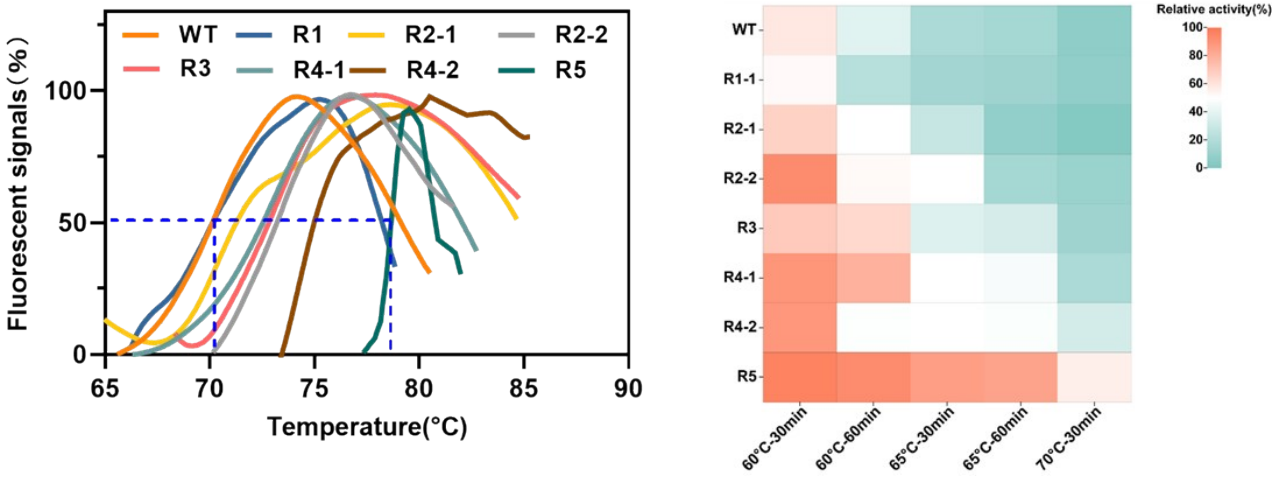

**Figure S5.** Characterization of WT and variant R5 kinetic parameters. (A) Conventional and Inverse (B-D) Michaelis-Menten plots of WT and R5, tested at 55°C with different substrate concentrations or different enzyme concentrations. Detection of conventional kinetic parameters of WT and R5 using 1-naphthylpropionate as a soluble substrate. (B) Fixed enzyme concentration of 12 μM. (C) Fixed enzyme concentration of 37 μM. (D) Inverse Michaelis–Menten[8] experiments assay with PLA substrate concentration fixed at 10 g/L. The concentration of lactic acid monomers is detected using HPLC[5]. The experiment is conducted in triplicate. Data are expressed as the mean ± s.d. (standard deviation).

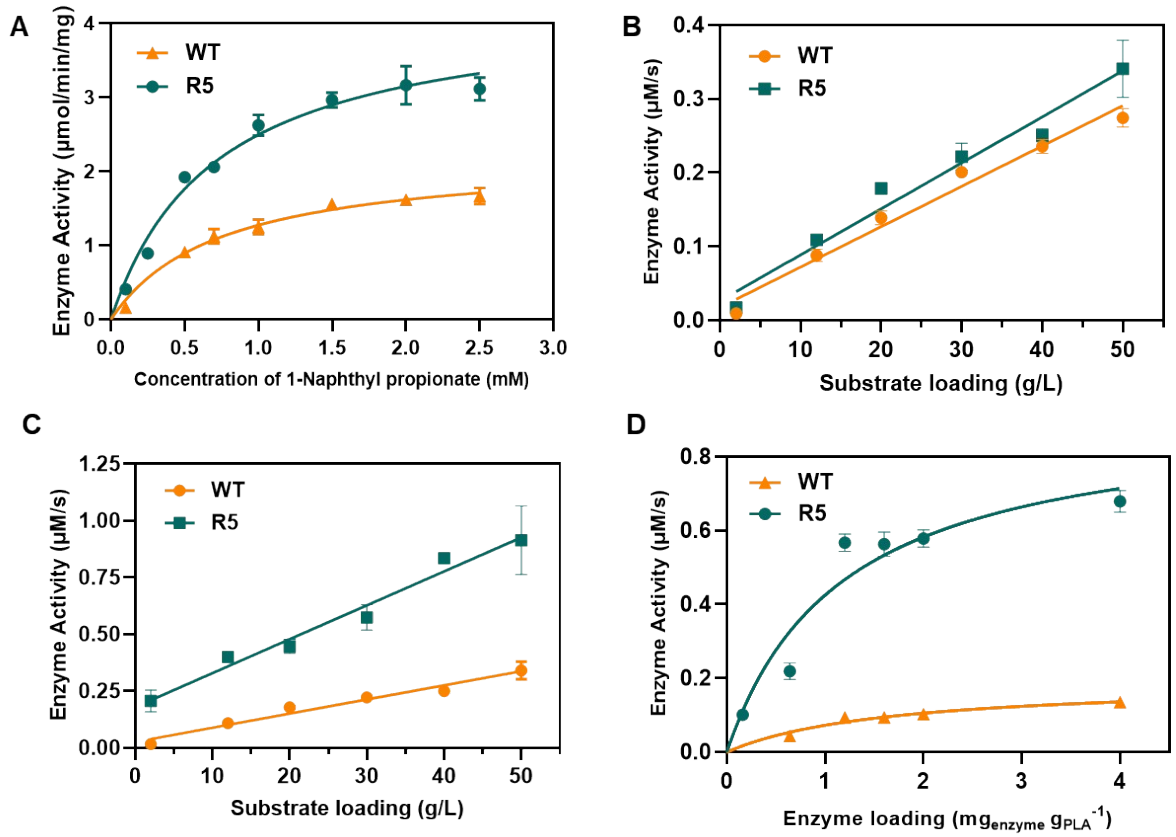

**Figure S6.** Substrate profiles for WT and variant R5 against model substrates. Model substrates include those commonly used for analyzing ester bond hydrolysis capability, such as p-nitrophenyl acetate (p-NPA, C2), p-nitrophenyl butyrate (p-NPB, C4), p-nitrophenyl hexanoate (p-NPH, C6), p-nitrophenyl octanoate (p-NPO, C8), p-nitrophenyl decanoate (p-NPD, C10), and 1-naphthyl propionate (C3). In addition, two other substrates were tested: tert-butyl (4-nitrophenyl) carbamate (p-NBC) containing a carbamate bond, and 4'-nitroacetanilide (p-NAA) containing an amide bond. Enzyme activity is defined as the amount of enzyme required to produce 1 μmol of para-nitrophenol (pNP) or 1-naphthol per minute at 55°C, serving as one unit of enzymatic activity.

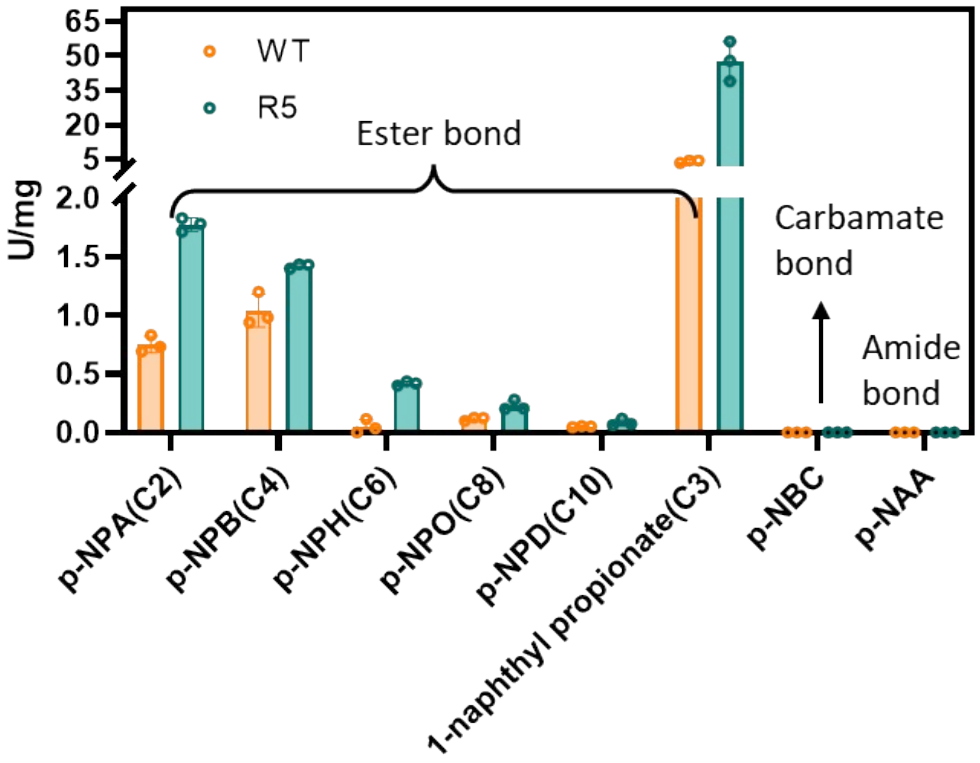

**Figure S7.** Structural alignment of the predicted structure of RPA1511 by AlphaFold2[12] with the crystal structure (PDB ID:4PSU[10]). The protein domains of predicted structure are shown as green cartoon and crystal structure as white cartoon. The missing 83-85 loop fragment is colored red. The Root Mean Square Deviation (RMSD) value between the two structures is only 0.21 Å.

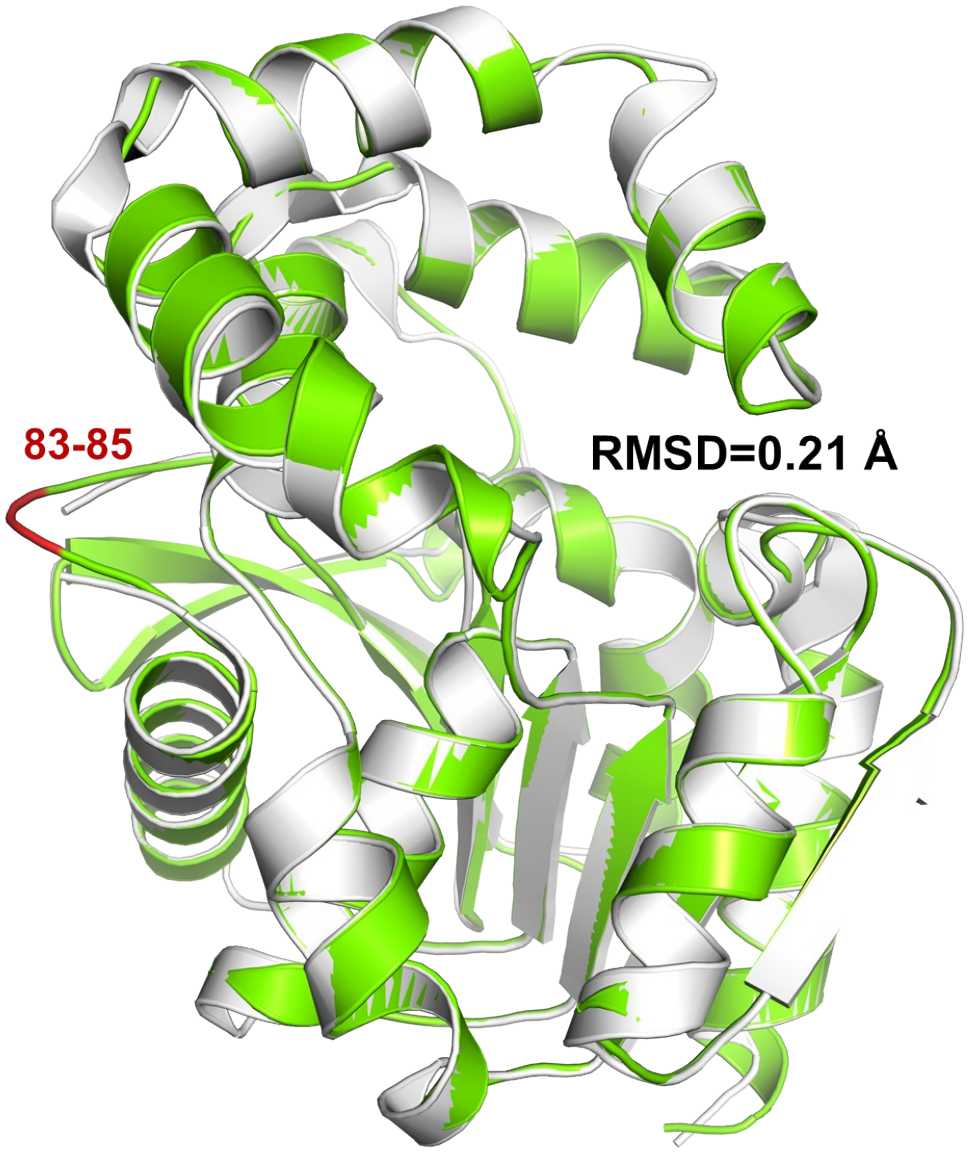

**Figure S8.** Comparison of the thermal stability of WT and the variant R5 based on MD simulations. (A) Mean root-mean-square fluctuation (RMSF) values for each residue over 100 ns. (B) The root-mean-square deviation (RMSD) values of the whole protein over 100 ns; (C) The radius of gyration (Rg) over 100 ns. (D) The solvent-accessible surface area (SASA) over 100 ns. Values correspond to the average of two independent 100 ns MD simulations.

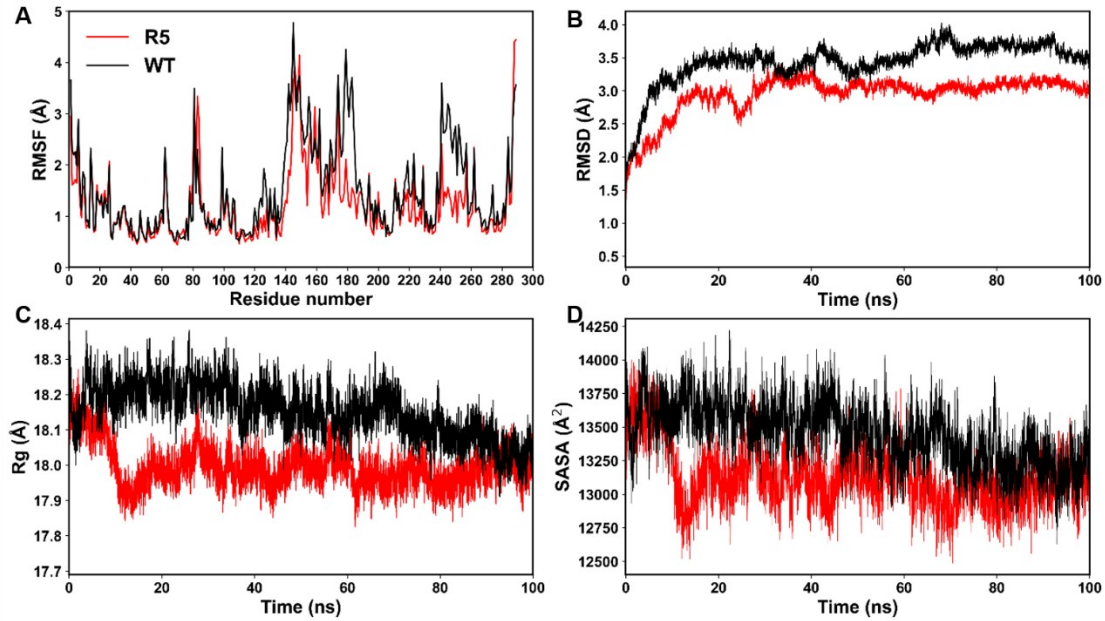


**Figure S9.** A single point mutation scan of V202 using the Rosetta cartesian_ddG method to calculate the $\Delta\Delta G_{fold}$(kcal/mol).

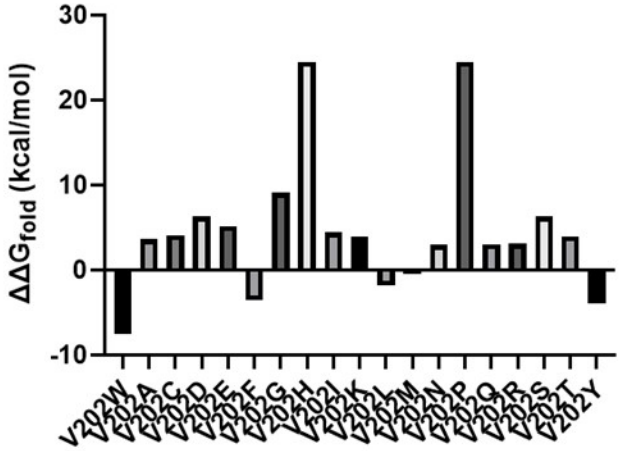

**Figure S10.** Structural formula of the model substrate 4LA marked with heavy atom names. $C_2$ atom is the tetrahedral center carbon attacked nucleophilically by S114 and set to $sp_3$ hybridization. The negative charge on the $O_5$ atom is neutralized by the oxyanion hole residues.

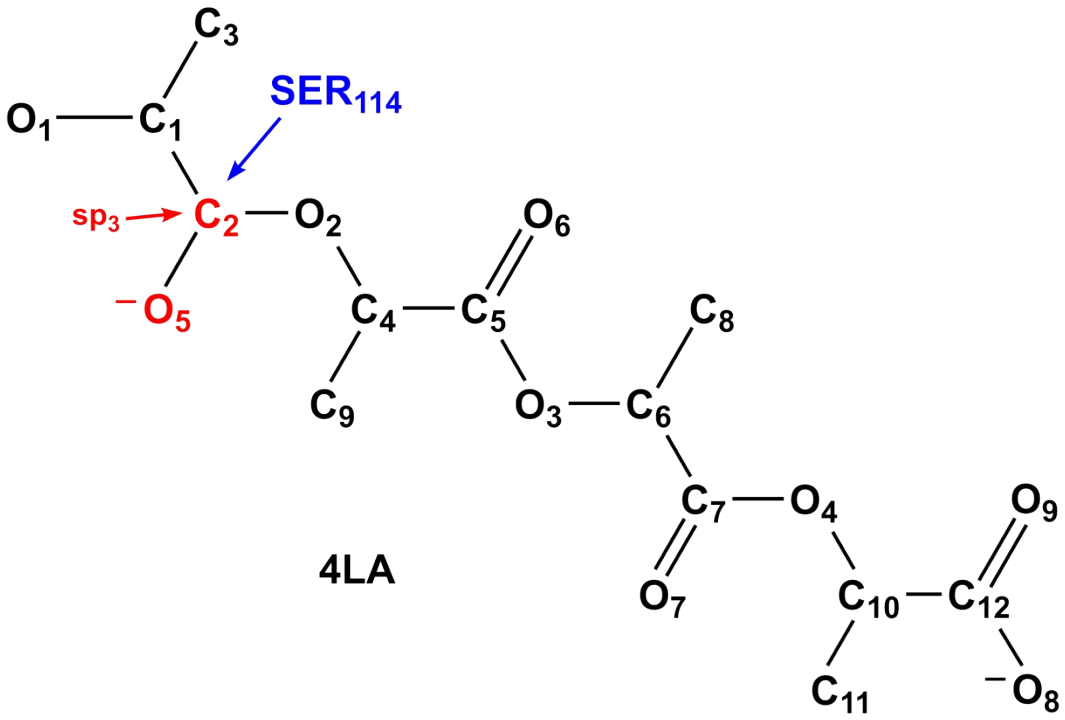

**Figure S11.** Scatter plots of the total score and atom distance constraint score of WT (A) and R5 (B) docking results computed by Rosetta.[13] The "total_score" represents the assessment of the total energy of docking models, while the "atom_pair_constraint" represents the penalty for the complex structure to be constrained.

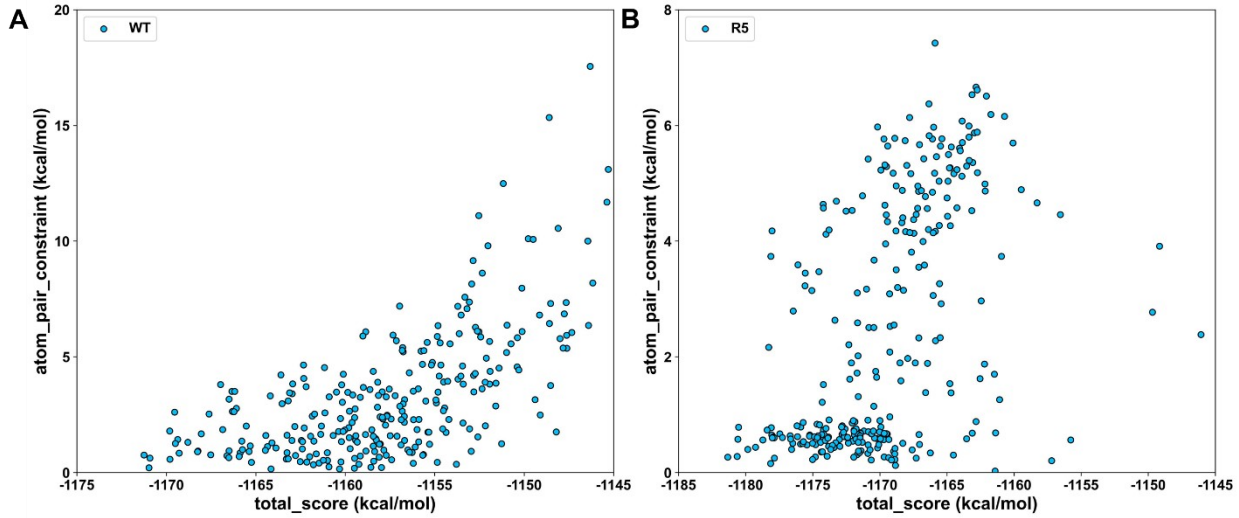

# References


1 J. J. Weinstein, A. Goldenzweig, S. Hoch and S. J. Fleishman, *Bioinformatics*, 2021, **37**, 123–125.

2 M. Musil, J. Stourac, J. Bendl, J. Brezovsky, Z. Prokop, J. Zendulka, T. Martinek, D. Bednar and J. Damborsky, *Nucleic Acids Res*, 2017, **45**, W393–W399.

3 Y. Cui, Y. Chen, X. Liu, S. Dong, Y. Tian, Y. Qiao, R. Mitra, J. Han, C. Li, X. Han, W. Liu, Q. Chen, W. Wei, X. Wang, W. Du, S. Tang, H. Xiang, H. Liu, Y. Liang, K. N. Houk and B. Wu, *ACS Catal.*, 2021, **11**, 1340–1350.

4 D. Suplatov, D. Timonina, Y. Sharapova and V. Švedas, *Nucleic Acids Res*, 2019, **47**, W308–W314.

5 L. Josef, H.-F. Julia, L. Daniel and L. Peter, *Bioinformatics*, 2016, **32**, 1414–1416.

6 X. Gao, X. Dong, X. Li, Z. Liu and H. Liu, *Sci Rep*, 2020, **10**, 10330.

7 H. Park, P. Bradley, P. Greisen, Y. Liu, V. K. Mulligan, D. E. Kim, D. Baker and F. DiMaio, *J Chem Theory Comput*, 2016, **12**, 6201–6212.

8 J. Kari, M. Andersen, K. Borch and P. Westh, *ACS Catal.*, 2017, **7**, 4904–4914.

9 H. Schägger and G. von Jagow, *Analytical Biochemistry*, 1987, **166**, 368–379.

10 M. Hajighasemi, B. P. Nocek, A. Tchigvintsev, G. Brown, R. Flick, X. Xu, H. Cui, T. Hai, A. Joachimiak, P. N. Golyshin, A. Savchenko, E. A. Edwards and A. F. Yakunin, *Biomacromolecules*, 2016, **17**, 2027–2039.

11 F. H. Niesen, H. Berglund and M. Vedadi, *Nat Protoc*, 2007, **2**, 2212–2221.

12 M. Mirdita, K. Schütze, Y. Moriwaki, L. Heo, S. Ovchinnikov and M. Steinegger, *Nat Methods*, 2022, **19**, 679–682.

13 G. Lemmon and J. Meiler, *Methods Mol Biol*, 2012, **819**, 143–155.